

Measurement Based Time-Domain Power Saving Through Radio Equipment Deactivation on Sub-6GHz Base Station Site

Youssef Agram*, François Rottenberg†, and François Quitin*

*Brussels School of Engineering, ULB, Brussels, Belgium

†Faculty of Engineering Technology, KULeuven, Ghent, Belgium

e-mail: *{youssef.agram, francois.quitin}@ulb.be,

†{francois.rottenberg}@kuleuven.be

Abstract—The paper presents a methodology for reducing the power consumption of radio access networks by scheduling the use of radio equipment from multiple radio access technologies while keeping comparable quality of service. Although 5G New Radio (NR) is known to be more energy-efficient than legacy 4G Long Term Evolution (LTE) equipment, previous work shows a higher static power for 5G-NR equipment using active antennas. In the context of increasing data traffic and the deployment of 5G-NR equipment along 4G-LTE, the question of concurrent energy-efficient use of these two technologies for a given traffic load arises. This analysis relies on on-site measurements from a macro sub-6GHz base station in Belgium, evaluating the energy efficiency of 4G-LTE and 5G-NR radio units. Our findings demonstrate that the 5G-NR equipment is more energy-efficient at higher traffic levels, i.e., ≥ 150 Mbps, while using 4G-LTE is preferable at lower traffic due to its smaller static power consumption. Besides, the dynamic energy-efficiency is 3 to 9 times higher for 5G-NR compared to 4G-LTE. The paper also proposes several radio unit deactivation scenarios: 1) using 4G-LTE radio units only and redirecting traffic on 5G-NR when reaching 80% of the maximum 4G-LTE capacity, 2) using 5G-NR radio units exclusively, and 3) dynamically selecting between 4G-LTE and 5G-NR based on the computed downlink data traffic threshold. The results show that Scenario 3 achieves the largest energy savings, reducing power consumption by 31.5% at the base station level. This paper demonstrates that it is possible to significantly reduce the energy footprint with equipment that are currently deployed.

Keywords—power consumption; base station; measurements; deactivation; radio units.

I. INTRODUCTION

The Radio Access Network (RAN) plays a critical role in mobile communications, including a large number of Base Stations (BSs) which are responsible for over 80% of the total energy consumption in mobile networks [1][2]. In addition, historical trends indicate that RAN energy consumption is still increasing, requiring concrete action from mobile operators who are constrained to reduce their carbon footprint and ensure compliance with climate targets [3][4][5]. Besides, 5G New Radio (5G-NR) infrastructures are being widely deployed, offering enhanced features designed to improve both quality of service and energy efficiency. These features include deeper sleep modes, leaner carrier design, higher bandwidth, etc., when compared to their legacy counterparts [6][7]. Whereas multiple Radio Access Technologies (RATs) add extra layers of complexity to power consumption handling, the concurrent operation of 4G Long Term Evolution (4G-LTE) and 5G-NR

equipment within existing RANs also presents a new set of challenges and degrees of freedom for energy savings [7]. While 5G technology is recognized for its superior energy efficiency at high traffic loads, it also exhibits a higher static power consumption compared to 4G-LTE at lower traffic levels [8]. This complementarity necessitates a strategic approach to schedule the dual-use of 4G-LTE and 5G-NR equipment from an energy-aware perspective, leveraging the strengths of each technology, without compromising the quality of service provided to end-users. Meanwhile, time-domain power saving features seem to provide the highest power saving gains [6].

Figure 1 shows on-site measured average Radio Frequency (RF) power consumption as a function of the average physical resource load for 2 Radio Units (RU) running different protocols, i.e., 4G-LTE for the Remote Radio Unit (RRU) and 5G-NR for the Active Antenna Unit (AAU). The intersection between the linear extrapolated trends indicates that it would be more energy-efficient to use one radio equipment rather than the other depending on the physical load, i.e., the 4G-LTE RRU at low and 5G-LTE AAU at high loads. It is, however, important to emphasize that this threshold does not correspond to the same service provided by both RUs. In fact, both have a different maximum capacity, e.g., bandwidth, number of layers, etc., and therefore, will not deliver the same downlink data traffic, even when the load is identical.

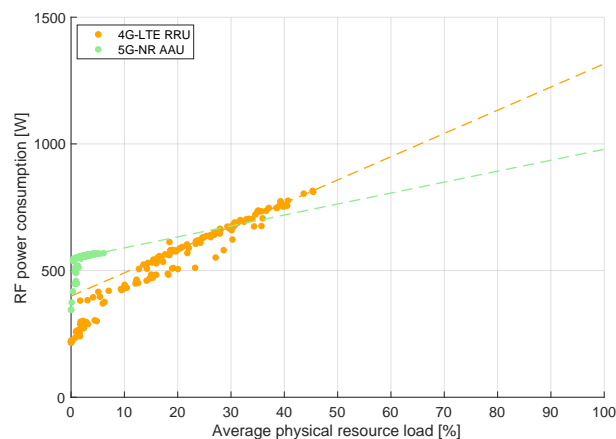


Figure 1. Average power consumption vs. average physical resource load measurements on an hourly basis. Inflexion of the curve is due to implemented power-saving modes [8].

This work aims to derive a simple energy-aware mechanism which deactivates specific RUs based on the downlink data rate, requested to the base station by User Equipments (UEs). This analysis assumes that UEs are both 4G-LTE and 5G-NR compatible. The purpose is also to compare energy-efficiency of equipment from both technologies and to quantify the energy savings achieved through the implementation of such mechanism.

This paper is organized as follows. Section II describes the architecture of the base station of interest, as well as the type and structure of available data. Section III recalls the BS power model from previous work, presenting a generic linear power consumption model for RUs, as a function of the physical resource load. Analysis and computation of the downlink data rate are performed in Section IV, before showing the relationship between power consumption and data traffic for all RUs. The implementation of the power saving mechanism through RU deactivation is illustrated in Section V, where several scenarios are proposed. Section VI concludes this work and lists future ones.

II. STRUCTURE OF THE BASE STATION

Measurements on which this study relies on are provided for an up-to-date 3-sector macro-BS deployed in a large city in Belgium. This site is equipped with 3 types of RUs:

- Radio Frequency Unit (RFU), installed in the BS cabinet and usually serving all 3 sectors at the same time,
- Remote Radio Unit (RRU), installed closer to passive antennas and dedicated to a specific sector,
- Active Antenna Unit (AAU), combining Analog Front-End (AFE), Power Amplifiers (PAs) and antenna elements in a single unit.

It supports three bands for LTE (i.e., 0.8, 1.8 and 2.1 GHz) and two bands for NR (i.e., 0.7 and 3.5 GHz). Figure 2 shows a simplified version of the BS architecture where each RU_i is enumerated with index $i \in \{1, 2, \dots, 8\}$. The Digital Baseband (DBB) performs digital signal processing operations and provides data and control signals to RUs using the Common Public Radio Interface (CPRI) [9][10][11]. The considered BS comprises two separate System Modules (SM). Power Supply and Cooling systems (PSC) are also installed on site but are not represented.

On-site measurements have been performed by mobile operators on an hourly basis over one week (6 days) in 2023. Several metrics are covered such as the number of used Physical Resource Blocks (PRB), the number of UEs having reported a Channel Quality Indicator (CQI) with index X_j , etc. The majority of those measurements are given per *cell*, i.e., per frequency band and per sector. Only power consumption is aggregated at the RU level. For confidentiality reasons, the raw dataset cannot be published.

III. POWER MODELS

Previous work already developed a detailed parametric model for the BS power consumption, expressed as sum of

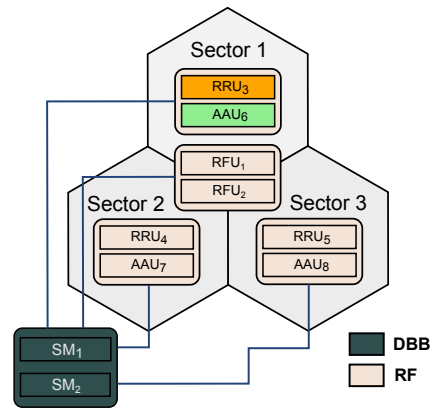


Figure 2. Simplified architecture of the base station of interest.

the main BS components [8][10]:

$$P_{BS} = \sum_{c=1}^{N_C} (P_{RU,c} + P_{DBB,c} + P_{PSC,c}), \quad (1)$$

where N_C denotes the number of cells and c the cell index (here and in the rest of this paper). It also demonstrates that RU equipment dominates in terms of power consumption. We will, therefore, be focusing on RUs in this study, which could themselves be split into the AFE and PAs. The average hourly RU power consumption can be expressed as:

$$\begin{aligned} \bar{P}_{RU}(T_k) &= \sum_{c=1}^{N_C} P_{PA}(\bar{x}_c(T_k); \chi_{PA,c}(T_k)) + P_{AFE}(\chi_{AFE,c}(T_k)) \\ &= \sum_{c=1}^{N_C} \alpha(\chi_{PA,c}(T_k)) \cdot \bar{x}_c(T_k) + \beta(\chi_{AFE,c}(T_k)) + P_{AFE}(\chi_{AFE,c}(T_k)), \end{aligned} \quad (2)$$

where T_k is the time sample corresponding to k^{th} hour on a given day. χ_{PA} and χ_{AFE} denote the set of configuration parameters for a given sub-component, e.g., number of active PAs, time ratio of downlink mode, etc., \bar{x}_c is the average load for a given cell, α and β the load-dependent and static PA power consumption. Expression (2) is linear with respect to the load, in line with Figure 1 and [12].

The average physical resource load for a given cell is itself given by:

$$\bar{x}_c(T_k) = \frac{\bar{N}_{PRB,c}(T_k)}{\bar{N}_{PRB,c}^{tot}(T_k)}. \quad (3)$$

$\bar{N}_{PRB,c}$ (respectively $\bar{N}_{PRB,c}^{tot}$) denotes the average used (respectively total available) number of PRBs.

The issue with the above equations is that they do not explicitly involve the data rate, which is a metric that reflects user data requests and Quality of Service (QoS). This will be addressed in the following section.

IV. DATA RATE ANALYSIS

The purpose of this subsection is to derive a relationship between the RU consumed power and the downlink data rate.

A. Computation

Data traffic computation can be confusing, given the complexity of 4G-LTE and 5G-NR protocols. In this case, the targeted traffic is that at the input of the physical layer. Even so, the data rate can be calculated in different ways depending on the technology, e.g., Transport Block Size (TBS) table in 4G-LTE [13]. However, an estimation of the instantaneous data rate per cell can be derived from [14]:

$$R_c^{5G}(t) = k_c \cdot N_{L,c} \cdot Q_m \cdot r \cdot \frac{N_{PRB,c}^\mu(t) \cdot 12}{T_s^\mu} \cdot (1 - OH^{5G}), \quad (4)$$

where $N_{L,c}$ is the supported number of layers in the cell, Q_m denotes the modulation order in bits/symbol, r is the code rate, OH the overhead due to PHY signaling and $N_{PRB,c}^\mu$ is the number of used PRB in the cell within T_s^μ , the duration of an OFDM symbol with given numerology factor μ . k_c is a scaling factor to adapt for MIMO layers, which is assumed to be 1 here [14]. The ratio $\frac{N_{PRB,c}^\mu \cdot 12}{T_s^\mu}$ represents the symbol rate, with 12 being the number of subcarriers contained in a 5G-NR PRB. $Q_m \cdot r$ is also known as the efficiency [13][15].

The above equation cannot be used as such to get an average data rate on an hourly scale for several reasons:

- it assumes a single efficiency factor. Yet, it is evident that thousands of user requests are sent per hour, each with a different channel quality. An hourly CQI distribution should, therefore, be considered, with $\mathbb{P}_c^i(X_j, T_k)$ being the probability of having CQI X_j , within hour T_k , on RU_i and cell c . CQI indexes X_j range from 0 to 15, leading to $N_{CQI} = 16$,
- the definitions of 4G-LTE and 5G-NR PRBs are different, 84 (respectively 12) subcarriers are contained in an LTE (respectively NR) PRB,
- a cell can itself be shared by multiple mobile operators, leading to multiple *logical cells*, denoted by index c' .

Assuming that every RU runs a single technology, the average downlink data rate for a given RU_i can thus be expressed as:

$$\bar{R}^i(T_k) = \sum_{c'=1}^{N_{C'}} \sum_{j=1}^{N_{CQI}} \alpha_{c'}^i \cdot Q_{m,j}^i \cdot r_j^i \cdot \frac{\mathbb{P}_{c'}^i(X_j, T_k) \cdot N_{PRB,c'}^i(T_k) \cdot N_s^i}{T_k}, \quad (5)$$

where $N_{C'}^i$ indicates the number of logical cells of RU_i and $\alpha_{c'}^i = N_{L,c'}^i \cdot (1 - OH^i)$. N_s^i denotes the number of subcarriers per PRB for a given technology running on RU_i . $Q_{m,j}^i$ and r_j^i are the modulation order and the code rate for a given CQI X_j and RU_i . Both depend on index i because 4G-LTE and 5G-NR RUs rely on different CQI standard tables, i.e., Table 7.2.3-1 (64QAM) for 4G-LTE [13] and Table 5.2.2.1-3 (256 QAM) for 5G-NR [15].

Note that one should, in theory, consider the Modulation and Coding Scheme (MCS) rather than the CQI to compute the efficiency. In fact, the scheduler could be using link-adaptation and lower the MCS to ensure an even lower Block Error Rate

(BLER) [16][17]. Unfortunately, the chosen MCS counters are not given in the data source. Useful RU technical parameters are given in Table I. All RUs are single-band except 4G-LTE RRUs, which are dual-band.

B. Results

The initial analysis focus on examining the average CQI distribution per RU. For this purpose, the average Cumulative Density Function (CDF) is calculated over the week as such:

$$F(X) = \sum_{j=1}^N \frac{1}{N_K} \sum_{k=1}^{N_K} \mathbb{P}(X_j, T_k), \quad (6)$$

where $N_K = 144$, the number of samples over 6 days. The CDFs are given in Figure 3. Since 4G-LTE and 5G-NR RUs rely on different CQI tables, it is necessary to project CQIs on the same table to make curves comparable. This is achieved by converting CQI indexes of each table into Signal-to-Noise Ratio (SNR), using appropriate relationships [19]. The results show that users served by 5G-NR RUs, on average, send a higher CQI back to the BS, indicating a higher channel quality. Several explanations are conceivable for such results: these could be due to a scheduler selection bias which intentionally selects UEs with higher SNR for 5G-NR, or to closer location of 5G-NR with respect to the BS, or to UEs with more robustness against interference.

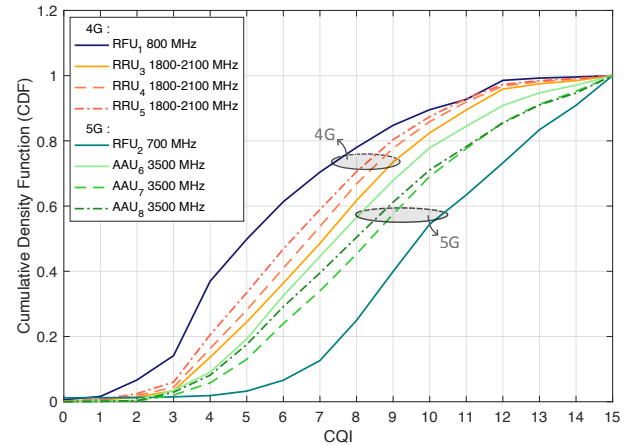


Figure 3. Average cumulative density function of reported CQI over the week (6 days), from Table 5.2.2.1-3 (256 QAM) [15].

Now, let us consider the relationship between the RU power consumption and the downlink data rate. Combining (2), (3) and (5) would lead to a linear relationship between \bar{R} and \bar{P}_{RU} , since they all linearly scale with the number of used PRBs. This is in fact what is shown in Figure 4.

The slopes on this graph represent the dynamic energy intensity in J/Mb, which corresponds to the inverse of the energy efficiency in Mb/J. It mainly depends on the average channel quality and on the RU capacity, i.e., $C = N_L \cdot B$, with B representing the bandwidth. Although they have the same theoretical capacity, RFU_1 has a lower energy efficiency

TABLE I. RU TECHNICAL AND MODEL PARAMETERS.

| RU type | Technology | f^1 [GHz] | $B_{C'}^2$ [MHz] | N_S^3 | $N_{C'}$ | $N_{L,c'}$ | N_s | OH | α [J/Mb] | P_{stat} [W] |
|------------------------|------------|----------------|---------------------|---------|----------|------------|-------|-------------------|--------------------|-------------------|
| RFU ₁ | LTE | 0.8 | 10 | 3 | 6 | 2 | 84 | 0.11 ⁴ | 5.1 | 373 |
| RFU ₂ | NR | 0.7 | 10 | 3 | 6 | 2 | 12 | 0.14 ⁵ | 1.5 | 275 |
| RRU _{3,4,5} | LTE | 1.8 2.1 | 20 | 1 | 4 | 44 | 84 | 0.11 ⁴ | 1.8 | 345 |
| AAU _{6,7,8} | NR | 3.5 | 100 | 1 | 2 | 4 | 12 | 0.14 ⁵ | 0.2 | 548 |

¹ Carrier frequency ² Bandwidth ³ Number of served sectors ⁴ [18] ⁵ [14]

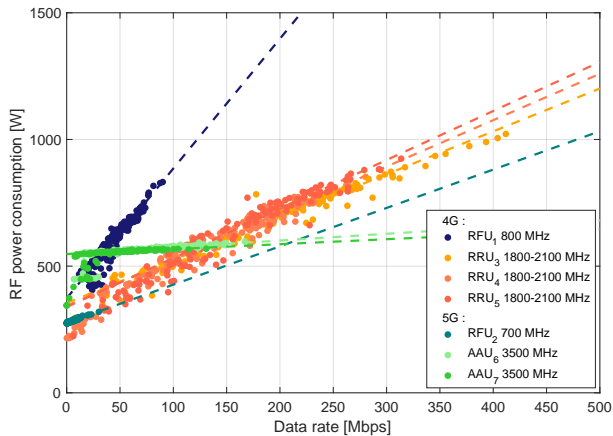


Figure 4. RU power consumption vs. data rate. Dashed lines represent linear regression models of scatter plots.

than RFU₂, due to its poorer average CQI distribution. Furthermore, AAUs have a very good energy efficiency, due to the combination of a higher capacity and a better channel quality. The absolute values indicate that AAUs should be preferred to RRUs at higher data rates regarding their lower power consumption, and vice versa. Note that AAU₈ is not shown due to a problem with power measurement that week. The dynamic energy intensities and static power values, denoted by α and P_{stat} are shown in Table I. It shows 3 to 9 times higher dynamic energy efficiency for 5G-RUs compared to its 4G-LTE counterparts.

In the next section, we examine how to leverage these results to implement our power reduction mechanism.

V. POWER SAVINGS THROUGH DEACTIVATION

This section proposes a radio equipment time-domain deactivation methodology and provide gain margins at the base station level for different mechanisms.

A. Methodology

The previous results validated the need to develop a power reduction mechanism. Several type of power-saving features exist and can be implemented, such as [6][8]:

- time-domain technique: switching of components from working to idle or sleep mode,
- frequency-domain technique: deactivation of a half or full frequency band,
- spatial-domain technique: deactivation of half of the layers and of the corresponding PAs and TX/RX chains,

- power-domain technique: reducing PA transmission power and PA efficiency improvement.

Here, we only focus on time-domain power-saving technique on a larger time scale, i.e., hourly, by switching-off radio equipment corresponding to one technology at a time. The users connected to these RUs must therefore be redirected to other active devices. The followed methodology includes some constraints and assumptions:

- 1) UEs should be rerouted on a RU that belongs to the same sector as the previous one, to prevent deteriorating the channel quality,
- 2) UEs should remain in the same band types, i.e., coverage bands ({700, 800} MHz) or high-bands ({1800, 2100, 3500} MHz), to prevent deteriorating the channel quality,
- 3) UEs must preserve their SNR and thus their CQI when redirected,
- 4) UEs are assumed to be both 4G-LTE and 5G-NR compatible,
- 5) a deactivated RU still consumes some residual power due to part of the AFE used to reactivate it by the DBB [8].

To satisfy the first 2 constraints, let us denote \mathcal{I} the set of all index pairs of RUs between which rerouting is feasible. Based on Figure 2, $\mathcal{I} = \{(1,2), (3,6), (4,7)\}$. Sector 3 is not considered in this section due to the lack of power measurements on AAU₈. From there, a decision threshold based on the total downlink hourly data rate is required. The linear regressions of Figure 4 cannot be used as such to find a threshold because the slope for each RU depends on the CQI distribution reported by the users connected to it, which we know differs between RUs. Projecting the data rate between pairs of RUs would change the average user's CQI, which would violate the 3rd constraint.

One solution is to build a global linear regression model, where each RU model also takes into account the CQI of the one with which it is paired. Such model can be expressed in matrix form:

$$\begin{bmatrix} \overline{P}_{RU_i} \\ \overline{P}_{RU_j} \end{bmatrix} = \begin{bmatrix} \alpha_i(\mathbb{P}^i(\mathbf{X}, \mathbf{T})) & \alpha_i(\mathbb{P}^j(\mathbf{X}, \mathbf{T})) \\ \alpha_j(\mathbb{P}^i(\mathbf{X}, \mathbf{T})) & \alpha_j(\mathbb{P}^j(\mathbf{X}, \mathbf{T})) \end{bmatrix} \cdot \begin{bmatrix} \overline{R}^i(\mathbb{P}^i(\mathbf{X}, \mathbf{T})) \\ \overline{R}^j(\mathbb{P}^j(\mathbf{X}, \mathbf{T})) \end{bmatrix} + \begin{bmatrix} \overline{P}_{stat}^i(\mathbb{P}^i(\mathbf{X}, \mathbf{T})) \\ \overline{P}_{stat}^j(\mathbb{P}^j(\mathbf{X}, \mathbf{T})) \end{bmatrix}, \quad (7)$$

with $(i, j) \in \mathcal{I}$, where $\alpha_i(\mathbb{P}^j(\mathbf{X}, \mathbf{T}))$ representing the model slope of RU_{*i*}, using the CQI distribution of RU_{*j*}, and \overline{P}_{stat}^i

being the static consumed power of RU_i . This model thus corresponds to 2 planes, whose intersection provides the decision threshold. An example is shown with pair (3,6) in Figure 5.

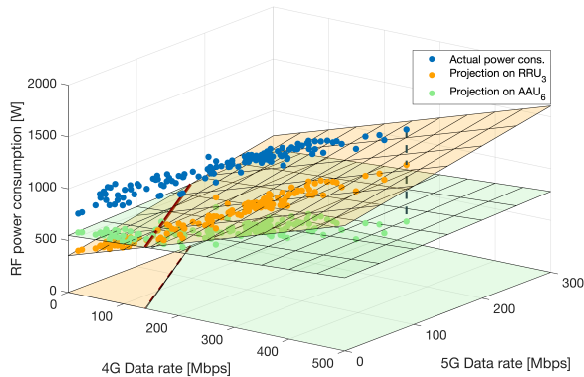


Figure 5. Power projection on models for RU pair (RRU₃, AAU₆).

The blue scatter points represent the actual total consumed power where both RUs are active, while orange and green points represent its projection on the 4G and 5G RU models, respectively. The intersection between these two model planes is given by the red straight line. It corresponds to the decision threshold locus, which separates the domain in two regions. The green (respectively orange) region indicates where is favorable from an energy point of view to reroute users to a 5G-AAU (respectively a 4G-RRU).

B. Results

The results of this implemented mechanism on the pair (3,6) are illustrated on Figure 6 and Figure 7. Figure 6 corresponds to the current situation, where both RUs are active, showing the average data traffic on each RU and its contribution to the total power consumption over the week on an hourly basis. Figure 7 is obtained applying the mechanism described above. Colors indicate the equipment to which the total data traffic is redirected. It shows a significantly reduced power consumption with the 5G-RU active most of the time. The only time the 5G-RU is switched-off in favor of the 4G-RU is at night, i.e., between 3 and 8 a.m. Note that the AFE’s contribution is also visible for both technologies, and that the power consumption remains relatively flat, thanks to the higher energy-efficiency of the 5G-AAU.

The last step aims to benchmark the above power saving mechanism with other deactivation scenarios by quantifying the energy savings for the entire BS over one week. For that purpose, several scenarios are considered in the benchmark:

- **Actual:** current situation where all RUs are running,
- **Scenario 1:** hourly deactivation of 4G-LTE RUs and redirecting data traffic on 5G-NR RUs, if total data traffic reaches 80% of the maximum capacity of the 4G-LTE RU. Maximum capacity can be computed using (5) and considering N_{PRB}^{max} ,
- **Scenario 2:** hourly deactivation of 4G-LTE RUs and redirecting all data traffic on 5G-NR RUs,

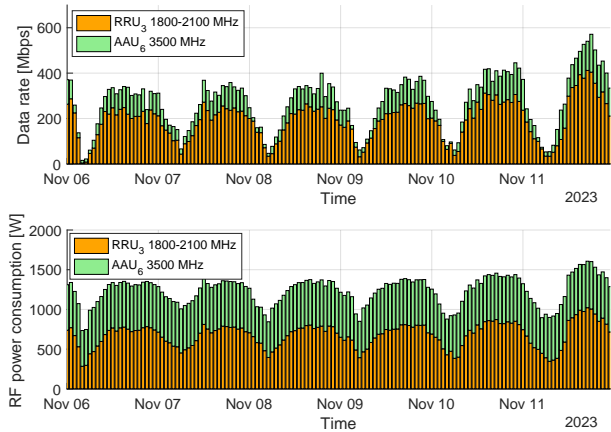


Figure 6. Power and total average data rate vs. time over a week in current situation.

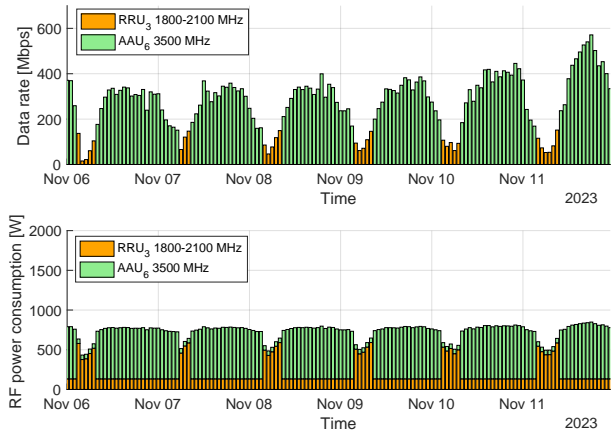


Figure 7. Power and total average data rate vs. time over a week when applying Scenario 3.

- **Scenario 3:** hourly deactivation of 4G-LTE RUs or 5G-NR RUs based on minimum power threshold criterion, as described previously.

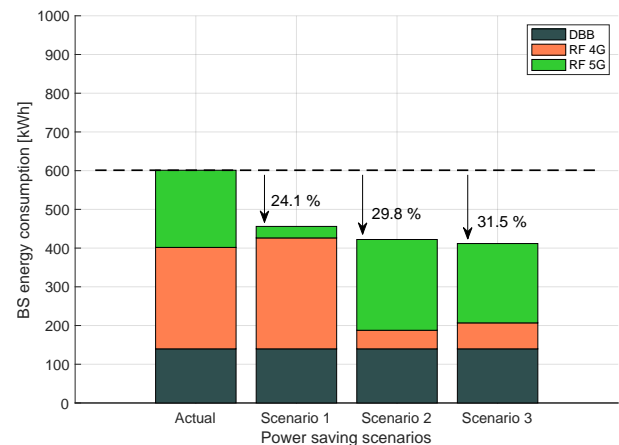


Figure 8. Benchmark of the energy savings for the entire BS over a week for different scenarios.

The results are given in Figure 8. Scenario 1 already shows a

power reduction of 24.1% with 4G-LTE almost always active, meaning that it rarely reaches 80% of its maximum capacity. Scenario 2 provides an even larger power reduction with 29.8% using 5G-NR only. Finally, Scenario 3 shows a slightly lower power consumption of 31.5% by switching between 4G-LTE and 5G-NR, following the methodology described above.

VI. CONCLUSION AND FUTURE WORK

This paper presents an on-site analysis of power consumption of radio equipment, providing a methodology for reducing the power usage by dynamically deactivating RUs based on the average data traffic on an hourly basis. Our findings reveal that 5G-NR RUs demonstrate 3 to 9 times higher dynamic energy efficiency compared to its 4G counterparts.

The core contributions of this study include the extension of existing power consumption models as a function of the downlink data rate. Those models are used to provide a time-scheduling for equipment use and shows that 5G-NR equipment should be privileged at higher traffic levels, i.e., ≥ 150 Mbps, while 4G-LTE equipment is preferable at lower levels, due to their smaller static power consumption. This work also proposes three scenarios for RU deactivation: 1) using 4G-LTE RUs only and redirecting the data rate on 5G-NR RUs when reaching 80% of maximum 4G-LTE capacity, 2) redirecting to 5G-NR RUs only, and 3) selecting between 4G-LTE and 5G-NR RUs based on the derived power consumption vs. data rate model. Our results indicate that Scenario 3 offers the largest power savings, achieving a 31.5% reduction in power consumption for the entire base station over a week. In contrast, the current situation is the most energy-consuming, when both technologies are used simultaneously.

These findings attest the potential for considerable energy savings using deployed radio equipment, while maintaining a comparable channel quality. The implications of our work are significant for current radio access network systems, where implementing intelligent RU deactivation may help mobile operators reducing energy and carbon footprints of their RAN, as well as their operational costs, without compromising user's QoS. Measurements and discussions with mobile operators reveal that some pieces of equipment are already partially deactivated during nighttime. All these results however assume that all UEs are both 4G-LTE and 5G-NR compatible, which is not yet the case in Belgium.

Future work should also consider other QoS metrics such as latency, as well as quantify the gain margin from integration of additional power-saving features, e.g., with lower time granularity. Finally, it is crucial to validate the assumption regarding the conservation of the channel quality for users under different deactivation scenarios.

ACKNOWLEDGMENT

The authors would like to thank Mwingz for their support.

REFERENCES

- [1] D. Lundén, J. Malmodin, P. Bergmark, and N. Lövehagen, "Electricity Consumption and Operational Carbon Emissions of European Telecom Network Operators," *Sustainability*, vol. 14, no. 5, p. 2637, 2022.
- [2] L. Stobbe *et al.*, *Umweltbezogene Technikfolgenabschätzung Mobilfunk in Deutschland (Environmental Technology Assessment of Mobile Communications in Germany)*, Umweltbundesamt, 2023.
- [3] L. Golard, J. Louveaux, and D. Bol, "Evaluation and projection of 4G and 5G RAN energy footprints: The case of Belgium for 2020–2025," *Ann. Telecommun.*, vol. 78, pp. 313–327, 2023.
- [4] "Green 5G: Building a sustainable world," *Analysys Mason*, Tech. Rep., Aug. 2020.
- [5] C. Freitag *et al.*, "The real climate and transformative impact of ICT: A critique of estimates, trends, and regulations," *Patterns*, vol. 2, no. 9, 2021.
- [6] T. Islam, D. Lee, and S. S. Lim, "Enabling Network Power Savings in 5G-Advanced and Beyond," *IEEE J. Sel. Areas Commun.*, vol. 41, no. 6, pp. 1888–1899, 2023.
- [7] D. López-Pérez *et al.*, "A survey on 5G radio access network energy efficiency: Massive MIMO, lean carrier design, sleep modes, and machine learning," *IEEE Communications Surveys & Tutorials*, vol. 24, no. 1, pp. 653–697, 2022.
- [8] L. Golard *et al.*, "A Parametric Power Model of Multi-Band Sub-6 Ghz Cellular Base Stations Using On-Site Measurements," in *Proceedings of the 2024 IEEE 35th Annual International Symposium on Personal, Indoor and Mobile Radio Communications (PIMRC)*, IEEE, 2024, pp. 1–7.
- [9] F. Launay and A. Perez, *LTE Advanced Pro: Towards the 5G Mobile Network*. John Wiley & Sons, 2019.
- [10] B. Debaillie, C. Desset, and F. Louagie, "A Flexible and Future-Proof Power Model for Cellular Base Stations," in *IEEE 81st Veh. Technol. Conf.*, 2015.
- [11] C. Desset, P. Wambacq, Y. Zhang, M. Ingels, and A. Bourdoux, "A flexible power model for mm-wave and thz high-throughput communication systems," in *2020 IEEE 31st Annual International Symposium on Personal, Indoor and Mobile Radio Communications*, IEEE, 2020, pp. 1–6.
- [12] A. Capone, S. D'Elia, I. Filippini, A. E. Redondi, and M. Zangani, "Modeling energy consumption of mobile radio networks: An operator perspective," *IEEE Wireless Communications*, vol. 24, no. 4, pp. 120–126, 2017.
- [13] 3GPP Technical Specification TS 36.213 V18.1.0, *Radio access network; Evolved universal terrestrial radio access (E-UTRA); Physical layer procedures (release 18)*, 2023.
- [14] 3GPP Technical Specification TS 38.306 V18.0.0, *Radio access network; NR; User Equipment radio access capabilities (release 18)*, 2023.
- [15] 3GPP Technical Specification TS 38.214 V18.1.0, *Radio access network; NR; Physical layer procedures for data (release 18)*, 2023.
- [16] F. J. Martín-Vega, J. C. Ruiz-Sicilia, M. C. Aguayo, and G. Gómez, "Emerging tools for link adaptation on 5G NR and beyond: Challenges and opportunities," *IEEE Access*, vol. 9, pp. 126 976–126 987, 2021.
- [17] E. Peralta, G. Pocovi, L. Kuru, K. Jayasinghe, and M. Valkama, "Outer loop link adaptation enhancements for ultra reliable low latency communications in 5G," in *2022 IEEE 95th Vehicular Technology Conference:(VTC2022-Spring)*, IEEE, 2022, pp. 1–7.
- [18] F. Rezaei, M. Hempel, and H. Sharif, "LTE PHY performance analysis under 3GPP standards parameters," in *2011 IEEE 16th international workshop on computer aided modeling and design of communication links and networks (CAMAD)*, IEEE, 2011, pp. 102–106.
- [19] Y. Wang, W. Liu, and L. Fang, "Adaptive modulation and coding technology in 5g system," in *2020 International Wireless Communications and Mobile Computing (IWCMC)*, IEEE, 2020, pp. 159–164.